J. Phys.: Condens. Matter **11** (1999) 3525–3534. Printed in the UK PII: S0953-8984(99)00897-8

Non-Fermi-liquid behaviour of $U_{3-x}Ni_3Sn_{4-y}$ single crystals

L Shlyk†‡, J C Waerenborgh§, P Estrela‖, L E De Long‡, A de Visser‖ and M Almeida§

† B Verkin Institute for Low Temperature Physics and Engineering, 47 Lenin Avenue, 310164 Kharkov, Ukraine

‡ Department of Physics and Astronomy, University of Kentucky, Lexington, KY 40506-0055, USA

§ Departamento Quimica, Instituto Tecnologico e Nuclear, P-2686 Sacavem Codex, Portugal

‖ Van der Waals–Zeeman Institute, University of Amsterdam, Valckenierstraat 65, NL-1018 XE Amsterdam, The Netherlands

Received 11 January 1999

Abstract. $U_3Ni_3Sn_4$ and $U_{2.9}Ni_{3.0}Sn_{3.9}$ single crystals exhibit a non-Fermi-liquid susceptibility $\chi \propto T^{-0.3}$ between 1.7 and 10 K. The electronic heat capacity coefficient $\gamma(T)$ of $U_{2.9}Ni_{3.0}Sn_{3.9}$ varies as the square root of temperature between 0.3 and 5 K. Although most available non-Fermi-liquid models are in disagreement with these results, the heat capacity data are consistent with a renormalization group calculation for magnetic fluctuations near an antiferromagnetic quantum critical point (QCP). Alternatively, both the magnetic and heat capacity data can be fitted to a Griffiths-phase model for magnetic clusters near a QCP, using a single characteristic exponent $\lambda = 0.7$.

1. Introduction

The behaviour of an increasing number of metallic, paramagnetic 4f- and 5f-electron systems are known to be inconsistent with simple Fermi-liquid theory. Although magnetic order is the typical ground state for rare-earth and actinide intermetallics, the ordering temperature of some materials is sensitive to f-state hybridization and can be driven to zero by varying composition or pressure. The suppression of magnetic order toward zero temperature may result in an extended 'non-Fermi-liquid' (NFL) regime in which critical fluctuations induce non-analytic temperature dependences of physical properties at temperatures $T < T_0$, where T_0 is a characteristic scaling temperature [1].

The $U_3T_3X_4$ compounds (T = transition metal, X = metalloid) with the cubic $Y_3Au_3Sb_4$ structure (a filled Th_3P_4 type) are good candidates for showing NFL behaviour, since they exhibit a range of unusual properties related to variations of 5f–ligand hybridization [2, 3]. The magnetic character of the uranium 5f electrons in these compounds may be suppressed by increasing hybridization of 5f conduction electrons via filling of the vacancies at the transition metal sites. For example, the stannides, $U_3T_3Sn_4$ (where T = Ni, Pt, Au) [3], do not exhibit long-range magnetic order down to 1.5 K, but are metallic and display heavy-fermion properties, except $U_3Cu_3Sn_4$, which is antiferromagnetic ($T_N = 12$ K).

A previous investigation [3] described a $U_3Ni_3Sn_4$ *polycrystal* as a moderately heavy fermion compound with an electronic heat capacity coefficient $\gamma = 92$ mJ K^{-2}/mol U, accompanied by saturating susceptibility and quadratic temperature dependence of the electrical resistivity below 10 K, characteristic of a *Fermi-liquid* ground state. In contrast,

0953-8984/99/173525+10$19.50

recent observations [4] reveal that the magnetic susceptibility χ of *single-crystal* $U_3Ni_3Sn_4$ has no tendency towards saturation for temperatures as low as 1.7 K. This is not surprising, since the physical properties of many uranium compounds are sensitive to metallurgical factors such as impurity concentration, phase distributions and structural defects. Therefore, we have grown single-crystal $U_3Ni_3Sn_4$ samples having slightly different starting compositions for extensive characterization via x-ray diffraction, transmission electron microscopy, electrical resistivity, thermopower, magnetic and heat capacity measurements.

Our data reveal that $U_{3-x}Ni_3Sn_{4-y}$ single crystals exhibit a novel form of NFL behaviour for a 5f system, including a square-root (as opposed to logarithmic) temperature dependence of the electronic heat capacity coefficient, similar to that previously observed only for $CeCu_2Si_2$ and $CeNi_2Ge_2$ single crystals [5].

Table 1. Details of the crystal structure refinement and crystal data for the two single crystals analysed.

Radiation, wavelength	Mo Kα, $\lambda = 0.71069$ Å	
Monochromator	Graphite	
Temperature	295 K	
ω–2θ scan	$\Delta\omega = 0.90 + 0.35 \tan\theta$	
Crystal-to-receiving-aperture distance	173 mm	
Horizontal, vertical aperture	4 mm, 4 mm	
Ideal chemical formula	$U_3Ni_3Sn_4$	
Ideal formula weight	5459.92 g mol^{-1}	
Crystal system	Cubic, body centred	
Space group	$I\bar{4}3d$ (No 220)	
μ (Mo Kα)	77.59 mm^{-1}	
Estimated chemical formula	$U_3Ni_3Sn_4$ (sample 2)	$U_{2.9}Ni_{3.0}Sn_{3.9}$ (sample 1)
a_0 (295 K)	9.3524(5) Å	9.3577(4) Å
V	818.03 Å	819.42 Å
Z	4	4
Approximate crystal dimensions (mm)	$0.07 \times 0.07 \times 0.25$	$0.13 \times 0.13 \times 0.03$
2θ range	2°–80°	2°–90°
Data set	$-16 \leqslant h \leqslant 16$	$0 \leqslant h \leqslant 18$
	$0 \leqslant k \leqslant 16$	$0 \leqslant k \leqslant 18$
	$0 \leqslant l \leqslant 16$	$0 \leqslant l \leqslant 18$
Total data	2481	1255
Unique data	422	437
Observed data	407	387
Number of refined parameters, p	10	11
Final agreement factors		
$R = \sum \|\|F_o\| - \|F_c\|\| / \sum \|F_o\|$	0.0565	0.0548
$wR_W = [\sum[w(F_o^2 - F_c^2)^2] / \sum[(F_o^2)^2]]^{1/2}$	0.1114	0.1297
GoF $= [\sum[w(F_o^2 - F_c^2)^2]/(n-p)]^{1/2}$	0.862	1.098

2. Sample preparation and structural characterization

Samples were prepared by induction melting two different charges with 3:3:4 or 3:2.8:4 atomic ratios of pure U (depleted), Ni and Sn, respectively. Single crystals were obtained by slowly cooling the charges in a semi-levitation, cold crucible. The resulting ingots were about 2–2.5 cm in diameter, and contained many single crystals with a maximum size of $3 \times 3 \times 3\ \mathrm{mm}^3$.

Single-crystal x-ray diffraction (XRD) data were collected at room temperature with an Enraf–Nonius CAD-4 diffractometer using graphite-monochromated Mo Kα radiation ($\lambda = 0.710\,69$ Å) and an ω–2θ scan mode. The measured intensities were corrected for Lorentz-polarization effects [6] and absorption by an empirical method based on ψ-scans [7]. The data, consistent with space group $I\bar{4}3d$, were refined assuming a $Y_3Au_3Sb_4$-type structure by a full-matrix, least-squares method [8] based on the squares of the structure factors. In the later stages of the refinement, the site occupation factors (SOF) were allowed to vary. Best-agreement factors $R = 0.0548$ and $R_W = 0.1297$, or $R = 0.0565$ and $R_W = 0.1114$, were obtained corresponding to the estimated compositions $U_{2.9}Ni_{3.0}Sn_{2.9}$ and $U_3Ni_3Sn_4$ (hereafter referred to as sample 1 and sample 2, respectively). Both estimated stoichiometries are consistent with the ideal composition, within experimental error (the standard deviations of the calculated SOF are $\leqslant$4%). The unit-cell parameters (9.3577(4) and 9.3524(5) Å for samples 1 and 2, respectively) were obtained by least-squares refinement of 25 reflections with $11^\circ < 2\theta < 45^\circ$. These estimated deviations from perfect stoichiometry correlate with an increase in lattice parameter, so ideal $U_3Ni_3Sn_4$ probably has the minimum unit-cell volume. A summary of the crystallographic data for the two single crystals analysed is given in table 1.

Specimens for examination by transmission electron microscopy (TEM) were prepared from pieces of sample 1. Flakes of thickness $\approx$120 μm were produced by crushing and placed

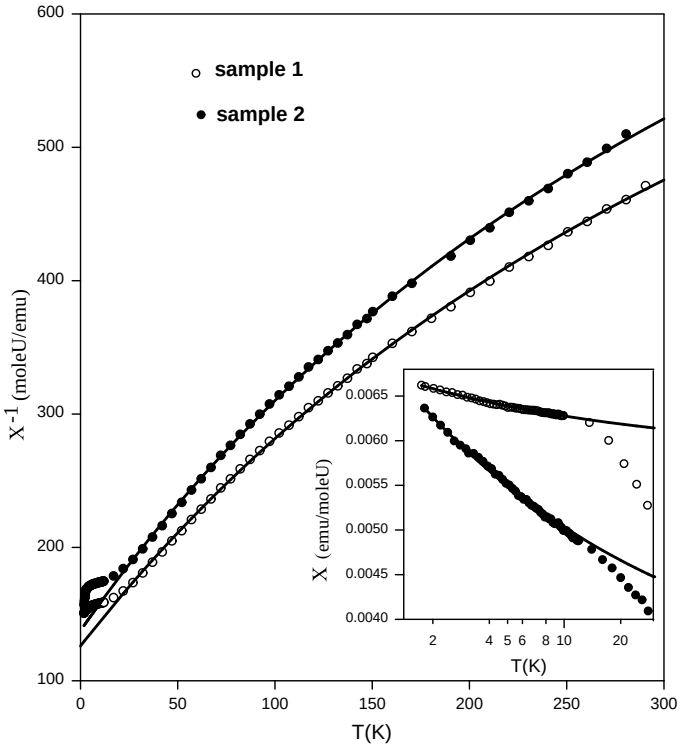

Figure 1. Inverse magnetic susceptibility χ^{-1} versus temperature T for $U_{2.9}Ni_{3.0}Sn_{3.9}$ (open symbols, sample 1) and $U_3Ni_3Sn_4$ (closed symbols, sample 2). Inset: low-temperature susceptibilities; the curves are fits to $\chi(T) \propto T^{-0.3}$.

on a Cu grid, and several electron diffraction patterns were taken over selected areas of a few μm^2. Careful examination of several samples revealed no foreign phases or splitting of the diffraction spots due to twinning. As point defects usually have dimensions smaller than the resolution of the electron microscope, we were not able to observe single vacancies. There was no evidence for superlattice reflections due to vacancy ordering.

3. Experimental results

DC magnetization and susceptibility measurements were performed over the temperature interval 1.7–300 K in applied fields up to 5 T using a Quantum Design MPMS5S SQUID Magnetometer. The temperature dependences of the magnetic susceptibilities of samples 1 and 2 follow a $T^{-0.3}$-dependence in the range 1.7–10 K (figure 1, inset). Above 25 K, the χ^{-1} versus T data approximately obey a modified Curie–Weiss law with Curie–Weiss temperature $\theta_p \approx -50$ (-60) K, effective moment $\mu_{eff} \approx 2.0$ (1.8) μ_B/U, and constant term $\chi_0 \approx 1.1$ (0.95) $\times 10^{-3}$ emu/mol U for sample 1 (2), in agreement with polycrystal results [3]. Sample 2 exhibits an overall magnitude of χ that is ≈10% below that of sample 1, as shown in figure 1. The reduction of μ_{eff} from 3.62 or 3.58 μ_B expected for U^{3+} or U^{4+} free ions, respectively, probably reflects the combined effects of the crystalline electric field and significant hybridization between 5f- and itinerant-electron states.

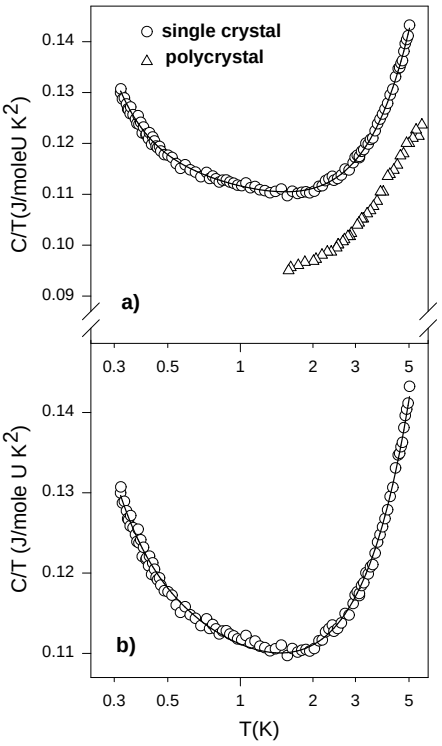

Figure 2. (a) Heat capacity C divided by temperature T for $U_{2.9}Ni_{3.0}Sn_{3.9}$ (sample 1) and polycrystalline sample data [3], versus log(T). The solid curve is a fit of the data to equation (1). (b) Heat capacity C divided by temperature T for $U_{2.9}Ni_{3.0}Sn_{3.9}$ versus log(T). The solid curve is a fit of the data to equation (3).

The heat capacity of sample 1 was measured in a ^{3}He cryostat using the relaxation method. The results are similar to polycrystal data [3] above 1.5 K (see figure 2(a)), but lower-temperature single-crystal data reveal a rapid increase in C/T between 0.3 and 0.7 K.

The heat capacity of sample 1 can be fitted (see figure 2(a)) with the following expression:

$$C = (\gamma_0 - \alpha\sqrt{T})T + \beta T^2 + D/T^2 \tag{1}$$

where $C_{el} = (\gamma_0 - \alpha\sqrt{T})T$ is the electronic contribution, $C_{lat} = \beta T^3$ is the lattice contribution and $C_{Sch} = D/T^2$ represents the high-temperature form of a nuclear Schottky term [9]. The best-fit coefficients are $\gamma_0 = 0.124$ J K^{-2}/mol U, $\alpha = 0.0151$ J K$^{-2.5}$/mol U, $\beta = 2.071 \times 10^{-3}$ J K^{-4}/mol U and $D = 4.622 \times 10^{-4}$ J K^{-1}/mol U. Using

$$C_{el} = n(12/5)\pi^4 R(T/\theta_D)^3$$

and $n = 10$ atoms per formula unit, we estimate a Debye temperature $\theta_D \approx 210$ K. The calculated electronic (C_{el}), lattice (C_{lat}) and Schottky (C_{Sch}) contributions to the total heat capacity divided by T versus temperature, according to equation (1), are shown in figure 3.

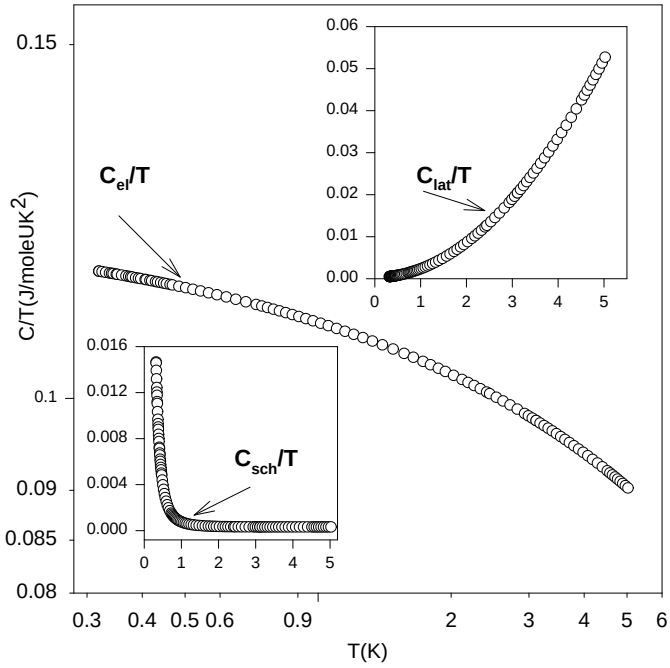

Figure 3. Calculated electronic (C_{el}), lattice (C_{lat}) and Schottky (C_{Sch}) contributions derived from best fits of the total heat capacity divided by T versus temperature, according to equation (1).

The nuclear heat capacity anomaly in paramagnetic, cubic $U_3Ni_3Sn_4$ can be attributed to atoms located at the $\bar{4}$- and 3-sites having axial symmetry; hence, isotopes having a non-zero quadrupole moment (i.e., having nuclear spin $I > 1/2$) may interact with the electric field gradient of neighbouring atoms. In addition, unpaired d or f electrons of Ni and U, respectively, can generate magnetic hyperfine fields if the atomic spin relaxation is slower than the Larmor frequency of the nuclear spin [5, 9–11]. Considering the natural abundances of relevant isotopes, only 1.2% of the Ni (^{61}Ni) and much less than 0.7% (^{235}U) of the depleted U may contribute to the nuclear Schottky term, assuming that it reflects both quadrupole and hyperfine interactions. Alternatively, ^{119}Sn comprises 9% of natural Sn, and could yield a dominant hyperfine contribution to the nuclear heat capacity. We estimate an *upper limit* (neglecting all nuclear contributions of the ^{61}Ni and ^{235}U isotopes) of the Sn-site hyperfine magnetic field of $|H_{eff}| = 240$ kG, which is several times larger than that determined from Mössbauer experiments on non-magnetic heavy-fermion materials [10, 11]. Considering the limiting assumptions made in deriving this estimate, it provides support for the credibility of our fits.

Renormalization group theory [12] predicts $\gamma \propto \gamma_0 - \alpha\sqrt{T}$ near a zero-temperature antiferromagnetic quantum critical point (QCP). The fitted value of

$$\alpha = (15/64)k_B N_A N[2/\pi T_0]^{3/2}\zeta(5/2)$$

allows us to estimate the characteristic temperature $T_0 \approx (10\ \mathrm{K}) \times N^{2/3}$. Assuming the N-dimensional bosonic order parameter $N = 1$, the best-fit value of $T_0 \approx 10$ K corresponds very well to the onset temperature of the non-analytic behaviour of $\chi(T)$ shown in the inset of figure 1.

Alternatively, self-consistent renormalized spin fluctuation (SCR) theory [13] also predicts a square-root form of the electronic heat capacity at low temperatures that evolves into a logarithmic behaviour, $C/T \sim \ln(T_0/T)$ at higher temperatures, and a good fit of the data was obtained using

$$C = \gamma_0 T \ln(T_0/T) + \beta T^3 + D/T^2 \tag{2}$$

with $\gamma_0 = 7.74 \times 10^{-3}$ J K^{-2}/mol U, $T_0 = 1.34 \times 10^6$ K, $\beta = 1.8 \times 10^{-3}$ J K^{-4}/mol U and $D = 3.79 \times 10^{-4}$ J K^{-1}/mol U. Multi-channel Kondo [14] or Kondo-disorder [15] models also predict a logarithmic dependence for $\gamma(T)$. The Kondo-disorder model demands $\chi(T) \propto -\ln T$, whereas the multichannel Kondo model can yield $\chi(T) \propto -T^{0.5}$ or $-\ln T$ at low temperatures. Fits to a $T^{-0.3}$-dependence yield slightly better results than the $-\ln T$ form, but are much better than the $-T^{0.5}$-fits (figure 4). However, the best-fit value of $T_0 \approx 10^6$ K derived from the heat capacity data is extremely high, and probably does not correspond to a physically significant spin-fluctuation energy.

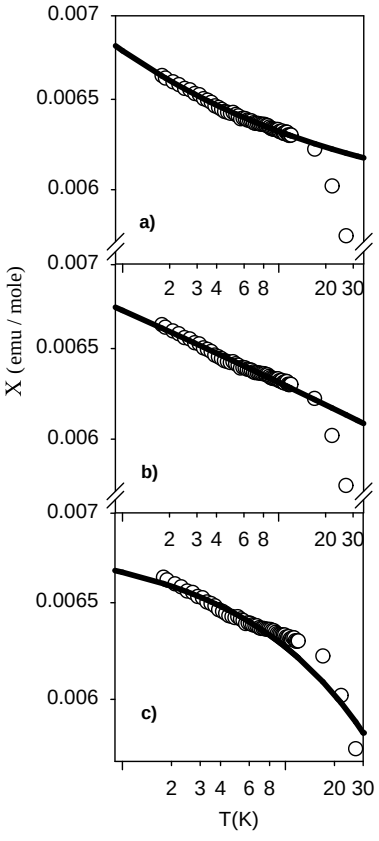

Figure 4. Low-temperature susceptibility for $U_{2.9}Ni_{3.0}Sn_{3.9}$ (sample 1); the curves are least-squares fits to: (a) $\chi(T) \propto T^{-0.3}$ (the Griffiths phase); (b) $\chi(T) \propto -\ln(T)$ (multichannel Kondo or Kondo-disorder models); (c) $\chi(T) \propto -T^{0.5}$ (the multichannel Kondo model).

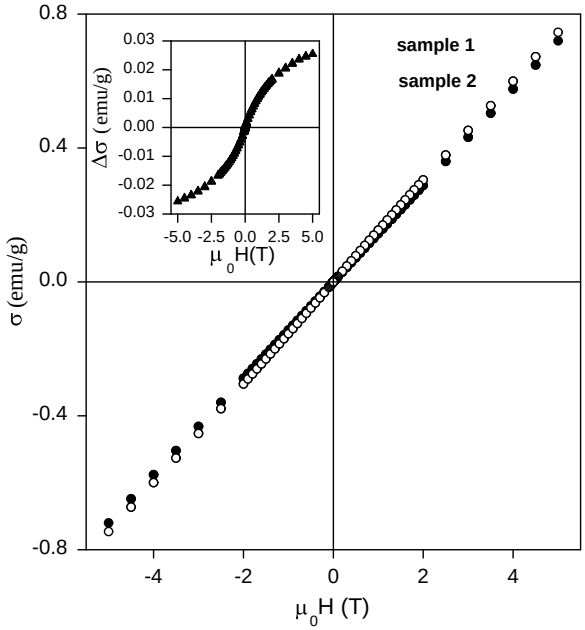

Figure 5. Magnetization $\sigma(H)$ versus magnetic field H at $T = 1.8$ K for $U_{2.9}Ni_{3.0}Sn_{3.9}$ (sample 1) and $U_3Ni_3Sn_4$ (sample 2). Inset: differences in magnetization $\Delta\sigma = \sigma_2 - \sigma_1$ of sample 1 and sample 2 versus H.

On the other hand, the $T \to 0$ behaviour of $\gamma(T)$ is also predicted to be of square-root form as a consequence of a zero-temperature quantum transition from a paramagnetic metal to a spin glass [16, 17], but the predicted [16] low-temperature susceptibility $\chi \propto -T^{3/4}$ is in conflict with our data. Nevertheless, it is conceivable that a small number of vacancies may lead to short-range magnetic order in a strongly correlated metal. The estimated increase in defect concentration of sample 1 (compared to sample 2) does not lead to pronounced differences in the overall behaviour of the susceptibility and magnetization (figures 1 and 5). However, defects apparently cause a clear reduction of the low-temperature $T^{-0.3}$-component of $\chi(T)$, as well as a small non-linear field dependence of the difference in magnetization $\Delta\sigma \equiv \sigma_1 - \sigma_2$ of the two samples (see the inset to figure 5). It is noteworthy that the non-linear component of the magnetization of sample 1 begins to saturate somewhere above $H_{sat} = 6$ T, which is also consistent with a characteristic temperature $T_0 \approx \mu_B H_{sat}/k_B > 4$ K, and corroborates the $\chi(T)$ and $C(T)$ data analysis.

The electrical transport data reveal a $T^{1.79}$-dependence of the electrical resistivity for $T < 12$ K (figure 6). The reduction of the resistivity exponent just below 2.0 is expected for an antiferromagnetic QCP, since the strong scattering of electrons takes place at particular antiferromagnetic wavevectors around the Fermi surface, allowing larger areas of Fermi surface to 'short out' this strong scattering with conventional Fermi-liquid transport [18]. The deviation of the data from this power law far above 10 K is therefore consistent with the Millis model and estimates of $T_0 \approx 10$ K derived from other physical properties. The thermoelectric power measurements performed by a differential method over the temperature range 16–300 K reveal a broad negative anomaly near $T = 175$ K, which is typical for spin-fluctuation systems (figure 7), and corresponds well with the lower limit of temperature for which $\chi^{-1} \propto T$ in figure 1.

Very recent experimental [19] and theoretical [20] work proposes that NFL behaviour is caused by competition between RKKY and Kondo interactions in the presence of atomic disorder, leading to a Griffiths phase (large magnetic clusters) close to a QCP. We find that the

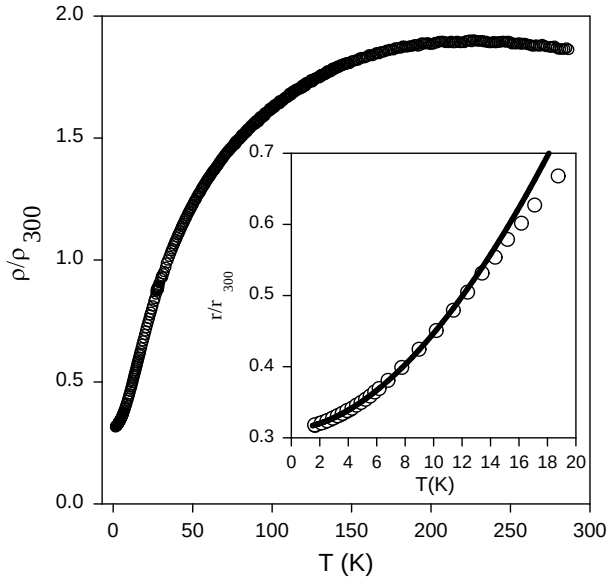

Figure 6. Normalized resistivity versus temperature for $U_{2.9}Ni_{3.0}Sn_{3.9}$ (sample 1). Inset: low-temperature resistivity; the solid curve is a least-squares fit of the data to $\rho(T) \propto T^{1.79}$.

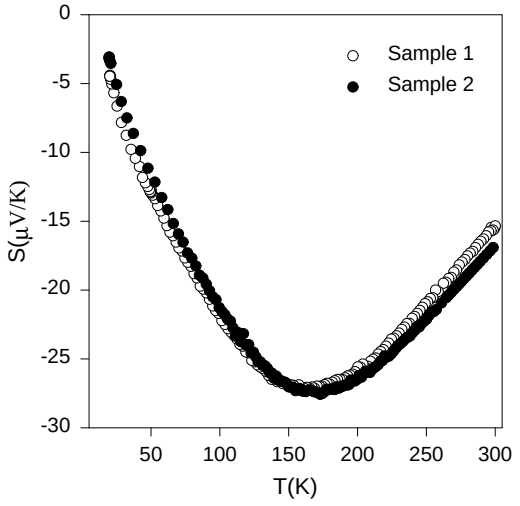

Figure 7. Thermopower $S(T)$ versus temperature for $U_{2.9}Ni_{3.0}Sn_{3.9}$ (open symbols, sample 1) and $U_3Ni_3Sn_4$ (closed symbols, sample 2) single crystals.

NFL behaviour of $C(T)$ and $\chi(T)$ in $U_{2.9}Ni_{3.0}Sn_{3.9}$ can be described by a divergent power law predicted by this model, i.e.,

$$C(T)/T \propto \chi(T) \propto \chi T^{-1+\lambda}$$

with $\lambda = 0.7$. We have obtained a good fit of the specific heat of sample 1 using

$$C = (\gamma_0 + \alpha T^{-0.3})T + \beta T^3 + D/T^2 \tag{3}$$

where $C_{el} = (\gamma_0 + \alpha T^{-0.3})T$ is the electronic contribution $C_{lat} = \beta T^3$ is the lattice contribution and $C_{Sch} = D/T^2$ represents the high-temperature form of a nuclear Schottky term [9] (figure 2(b)). The best-fit coefficients are $\gamma_0 = 0.0932\,\mathrm{J\,K^{-4}/mol\,U}$, $\alpha = 0.0159\,\mathrm{J\,K^{-1.7}/mol\,U}$, $\beta = 1.6421 \times 10^{-3}\,\mathrm{J\,K^{-4}/mol\,U}$ and $D = 2.5968 \times 10^{-4}\,\mathrm{J\,K^{-1}/mol\,U}$. These values show that the heat capacity contributions at $T = 5\,\mathrm{K}$ (or $T = 0.3\,\mathrm{K}$) are 72% (92%) fermionic, 28% (less than 1%) lattice, and less than 1% (7.6%) nuclear. Note that the calculated contributions are

only slightly different from those obtained above from renormalization group theory; for example, the *upper limit* (neglecting all nuclear contributions of the ^{61}Ni and ^{235}U isotopes) of the Sn-site hyperfine magnetic field $|H_{eff}| = 146$ kG (1.6 times less than the previous estimate) and the estimated Debye temperature is 228 K. We note that the renormalization group calculation yields slightly better agreement with the experimental heat capacity data over the temperature interval 0.6–1.7 K (compare figures 2(a) and 2(b)); nevertheless, the Griffiths-phase model provides a self-consistent description of the thermal and the magnetic data. The electronic (C_{el}), lattice (C_{lat}) and Schottky (C_{Sch}) contributions to the total heat capacity, as calculated according to equation (3), are displayed in figure 8.

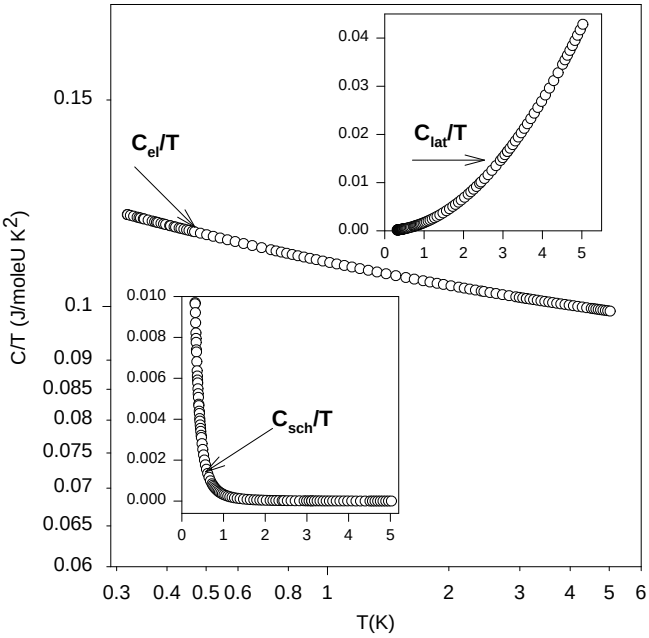

Figure 8. Calculated electronic (C_{el}), lattice (C_{lat}) and Schottky (C_{Sch}) contributions derived from best fits of the total heat capacity divided by T versus temperature, according to equation (3).

4. Conclusions

We have undertaken a thorough analysis of the heat capacity and susceptibility of $U_{2.9}Ni_{3.0}Sn_{3.9}$, and conclude that several NFL models (e.g., multichannel Kondo [14] and Kondo disorder [15]) commonly considered in the contemporary literature do not describe the entire data set known for this material. We find that satisfactory fits of the heat capacity data below 6 K always require a dominant electronic term that decreases weakly with increasing temperature, and a relatively small term having a T^{-2}-dependence, consistent with a Schottky anomaly present at lower temperatures. We obtain very similar estimates of the temperature-independent electronic heat capacity coefficient γ_0, the lattice heat capacity and the small nuclear Schottky term, independent of the details of the particular model employed. All attempts to include a logarithmic heat capacity term resulted in an unphysically high characteristic temperature scale $\approx 10^6$ K. We conclude that the electronic heat capacity coefficient exhibits a near-square-root temperature dependence, which previously has only been observed in two Ce systems [5], and differs from the typical logarithmic dependence reported for other U-based NFL systems [1].

Two models (Millis renormalization group and Griffiths-phase models), both of which

depend upon the existence of a low-temperature QCP between paramagnetic and magnetically ordered states, appear to be consistent with experiments to date. Millis's treatment does not include the effects of disorder, which might be present in our sample and in any other real system, while the Griffiths-phase model includes disorder as a crucial ingredient. Recent renormalization group predictions [18] for the susceptibility of a well-ordered material near antiferromagnetic QCP in the three-dimensional case yield $\chi \propto -T^{1.5}$, in conflict with our data, and may indicate that the low-temperature behaviour of the $\chi(T)$ is strongly affected by very small amounts of disorder.

The precise role of small amounts of disorder in the behaviour of $U_3Ni_3Sn_4$ must be investigated by further studies of carefully characterized samples with various stoichiometries. Additional lower-temperature studies of the behaviour of the heat capacity and magnetic susceptibility are under way to search for phase transitions, and obtain more precise estimates of the NFL power laws observed in the present study.

Acknowledgments

We thank Professor E Dickey for assistance in the transmission electron microscopy studies. The single-crystal samples were grown by LS during her stay in Portugal under the support of a NATO fellowship. Research at the University of Kentucky was supported by NSF Grant No INT-9515504. PE acknowledges the European Commission for a grant within the TMR Programme. We thank Professor M B Maple and Dr B A Jones for sending us preprints of unpublished work, and Professor A Castro-Neto and Professor A Millis for helpful discussions.

References

[1] Maple M B, Dickey R P, Herrmann J, de Andrade M C, Freeman E J, Gajewski D A and Chau R 1996 *J. Phys.: Condens. Matter* **8** 9773
[2] Endstra T, Nieuwenhuys G J, Mydosh J A and Buschow K H J 1990 *J. Magn. Magn. Mater.* **89** L273
[3] Takabatake T, Miyata S, Fujii H, Aoki Y, Suzuki T, Fujita T, Sakurai J and Hiraoko T 1993 *J. Phys. Soc. Japan* **59** 4412
[4] Shlyk L, Troc R, Waerenborgh J C, Paixao J A, Costa M M R and Almeida M 1996 *Proc. 26ièmes Journées des Actinides (Szklarska Poreba, Poland)* p 214
[5] Steglich F, Buschinger B, Gegenwart P, Lohmann M, Helfrich R, Langhammer C, Hellmann P, Donnevert L, Thomas S, Link A, Geibel C, Lang M, Sparn G and Assmus W 1996 *J. Phys.: Condens. Matter* **8** 9909
[6] Fair C K 1990 *MOLEN* Enraf–Nonius, Delft, The Netherlands
[7] North A C T 1968 *Acta Crystallogr.* A **24** 351
[8] Sheldrick G M 1993 *SHELXL-93: Program for Crystal Structure Refinement* University of Göttingen, Germany
[9] Lounasmaa O V 1967 *Hyperfine Interactions* (New York: Academic)
[10] Chevalier B, Fournes L and Etourneau J 1996 *Proc. 26ièmes Journées des Actinides (Szklarska Poreba, Poland)* p 66
[11] Polikarpov M A, Cherepanov V M, Chuev M A and Yakimovet S S 1994 *Physica* B **199/200** 45
[12] Millis A J 1993 *Phys. Rev.* B **48** 7183
Zülicke A and Millis A J 1995 *Phys. Rev.* B **51** 8996
[13] Moriya T and Takimoto T 1995 *J. Phys. Soc. Japan* **64** 960
[14] Cox D L and Jarrell M 1996 *J. Phys.: Condens. Matter* **8** 9825
[15] Miranda E, Dobrosavljevic V and Kotliar G 1996 *J. Phys.: Condens. Matter* **8** 9871
[16] Sengupta A M and Georges A 1995 *Phys. Rev.* B **52** 10 295
[17] Sachdev S, Read N and Oppermann R 1995 *Phys. Rev.* B **52** 10 286
[18] Millis A J 1998 Private communication
Ioffe L B and Millis A J 1995 *Phys. Rev.* B **51** 16 151
[19] de Andrade M C, Chau R, Dickey R P, Dilley N R, Freeman E J, Gajewski D A, Maple M B, Movshovich R, Castro Neto A H, Castilla G E and Jones B A 1998 *Phys. Rev. Lett.* **81** 5620
[20] Castro Neto A H, Castilla G E and Jones B A 1998 *Phys. Rev. Lett.* **81** 3531